



Kinetic study of the reaction of 2-aminobenzamid with 2, 6-dichlorobenzald-ehyde for producing 2-(2,6-dichlorophenyl)-2,3-dihydroquinazolin-4(1H)-one

Mehdi Shahraki*, Sayyed Mostafa Habibi-Khorassani and Fatemeh Fattahi

Department of Chemistry, University of Sistan and Baluchestan, P. O. Box 98135-674, Zahedan, Iran

ABSTRACT

Kinetic of the synthesis reaction of 2-(2, 6-dichlorophenyl)-2, 3-dihydroquinazolin-4(1H)-one in the presence of 2-aminobenzamid and 2, 6-dichlorobenzaldehyde has been spectrally investigated. For this purpose, parameters of the reactions were monitored by UV/vis spectrophotometry. Kinetics of the reaction including the effects of the amounts of 2, 6-dichlorobenzaldehyde, presence of maltose as a catalyst, temperature, and different polar solvents on the reaction rate were investigated in detail. Rational explanations to account for the unique results, especially for the temperature and solvent effects on the reaction rate, are also provided. A rate law consistent with the observed kinetic data and the proposed mechanism was suggested. In the PH range near or above neutrality imine formation in step₂ (rate constant (k_2) of reaction mechanism) was a rate determining step, but in the present work in the acidic pH range (formic or acetic acids) rate determining step is step₁ (k_1) of reaction mechanism, this confirmed based upon the steady state and the solvent studies on the reaction rate. In both solvent, the reaction was enthalpy controlled (ΔH^\ddagger is much greater than $T\Delta S^\ddagger$), never the less ΔS^\ddagger in the formic acid was less than a mixture of formic acid/ acetic acid, this imply that why the reaction occur more easily in the formic acid.

Keywords: Kinetics, Catalyst, Mechanism, Heterocyclic compound, 2, 3-dihydro-2-phenylquinazolin 4(1H)-one, maltose.

INTRODUCTION

Literature reports that quinazolinone moieties have been explored as key functional groups in a variety of anticancer agents. Many quinazolinones have contributed to the quest for an ultimate antitumor chemotherapeutic agent. 2, 3-dihydroquinazolin-4(1H)-ones (Fig. 1) shows promising antitumor potency [1].

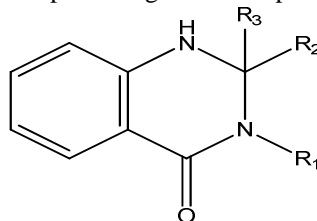


Fig. 1 2, 3-dihydroquinazolin-4(1H)-one

2,3-dihydroquinazolin-4(1H)-ones are known to possess diverse pharmacological properties [2–4]. Quinazolinones and their derivatives are an important class of N-heterocycles, of interest medicinal chemists due to their various biological activities such as hypnotic, sedative, analgesic, anticonvulsant antitussive, antibacterial, antidiabetic, anti-inflammatory, antitumor activities [5] and herbicidal agents, as well as plant growth regulators [6]. Certain DHQ derivatives may also have interesting features in their electronic spectra [5]. In addition, these compounds, as chemical intermediates, can easily be oxidized to their corresponding quinazolin-4(3H)-ones [7], which are also important biologically active heterocyclic compounds [8, 9]. Various works are devoted to the synthesis of quinazolin-4(3H)-ones either by oxidation of 2, 3-dihydroquinazolin-4(1H)-ones using suitable oxidizing agents

[10,11] or by various condensation procedures [12–16]. Many classical methods for the construction of 2, 3-dihydro-2-aryl-4(1H)-quinazolinones have been employed [17–19]. Several methods have been reported for the synthesis of 2, 3-dihydroquinazolinones. Among them, the most direct procedure includes condensation of the appropriate derivatives of anthranilamide with an aldehyde or ketone in the presence of Brønsted acid or Lewis acid [20–24]. Synthesis of this class of compounds has been carried out with different methods including a three-component coupling of isatoic anhydride, primary amines, and aldehydes with different catalysts [25-29]. In this paper, we report our kinetic study for the reaction of 2-aminobenzamide with 2, 6-dichlorobenzaldehyde at 293–308 K and atmosphere pressure using the relative rate coupled with spectrophotometric (UV/vis) technique. Literature reports that quinazolin- one moieties have been explored as a key functional group in a variety of anticancer agents. Previously, numerous kinetic investigations have been reported using this technique [30-39].

EXPERIMENTAL SECTION

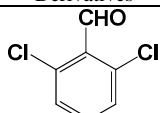
2.1 Chemicals and Apparatus Used

Starting reagents 2-aminobenzamide **1** (98%) and 2, 6-dichlorobenzaldehyde **2** (98%) and the solvents formic acid (99/5%) and acetic acid (99/5%) were obtained from Merck (Darmstadt, Germany) and used without further purifications. All spectra and kinetic measurements were recorded on a Cary UV/ vis spectrophotometer model Bio-300 with a 10 mm light-path quartz cell equipped with a water thermostat cell throughout the current work.

2.2 Synthesis of 2-(2, 6-dichlorophenyl)-2, 3-dihydroquinazolin-4(1H)-one

To evaluate the generality of the process, the method used for the synthesis of 2-(2, 6-dichlorophenyl)-2, 3-dihydroquinazolin-4(1H)-one was studied (**Table. 1**). The mixture of 2-aminobenzamide (1 mmol), 2, 6-dichlorobenzaldehyde (1 mmol) and formic acid (1 ml) was stirred at room temperature. After completion of the reaction (monitored by TLC), the reaction mixture was washed with H₂O. The residue was then recrystallized from EtOH to furnish the pure product 2-(2, 6-dichlorophenyl)-2, 3-dihydroquinazolin-4(1H)-one. For this reaction melting points were measured on an Electrothermal 9100 apparatus. Results have been shown in (**Table. 1**).

Table. 1 Synthesis of 2-(2, 6-dichlorophenyl)-2, 3-dihydroquinazolin-4(1H)-one using formic acid as a solvent and catalyst

| Entry | Derivatives | Time (hr) | Product | Mp (Obsd) (°C) |
|-------|---|-----------|----------|----------------|
| 1 |  | 2 | 3 | 195-197 |

RESULTS AND DISCUSSION

3.1 General Procedure

To investigate the mechanism of the reaction between 2-aminobenzamide and 2, 6-dichlorobenzaldehyde in the presence and absence of some catalyst, the kinetics were studied at different temperatures in formic acid as a solvent and catalyst. A conventional kinetic method for determining the values of rate constants was used. These reactions were studied spectrophotometrically. All reactions were conducted at 25 °C, except in those where the effects of temperature were investigated. The temperatures of the reaction mixtures were controlled throughout all kinetic experiments to ± 0.1 °C. All solutions were prepared by measuring the calculated amounts of substances in formic acid. The reactions were initiated by mixing equal volumes of 2-aminobenzamide and 2, 6-dichlorobenzaldehyde in the quartz cuvette. During all experiments the concentration of 2-aminobenzamide and 2, 6-dichlorobenzaldehyde was constant (1×10^{-2} M), except under pseudo-order conditions where the concentration of 2, 6-dichlorobenzaldehyde was (1×10^{-3} M). Spectral changes in the first experiment resulting from the mixing of 2-aminobenzamide (1×10^{-2} M) and 2, 6-dichlorobenzaldehyde (1×10^{-2} M), were recorded over a wavelength range of 200-500 nm as a suitable wavelength at which the kinetic experiments could be performed. The absorbance changes of the mixed solution were recorded in 2 minute interval during the whole reaction time at ambient temperature (**Fig. 2**). From this, the appropriate wavelength was discovered to be 420 nm. Since at this wavelength, reactants (**1**), (**2**) and intermediates have no relatively absorbance value, it provides the opportunity to fully investigate the kinetics and mechanism of the reaction. Hence, in the second experiment, the reaction was undertaken under same conditions at 420 nm and 25°C for recording absorbance curve against time (**Fig. 4**). As can be seen in **Fig. 3**, the original experimental absorbance curve versus time (dotted line) exactly fits the second order fit curve (solid line) [40]. So, the reaction is second order ($\alpha + \beta = 2$), and the general reaction rate is described by the kinetic equation:

$$\text{Rate} = k_{\text{ovr}} [\mathbf{1}]^{\alpha} [\mathbf{2}]^{\beta} \quad (1)$$

The second-order rate constant at 25°C ($k_{\text{ovr}} = 17.88 \text{ min}^{-1} \cdot \text{M}^{-1}$) is then automatically calculated using standard equations within the program [30].

3.2 Effect of Concentration

In the third experiment, in order to obtain the partial order of reaction regarding 2, 6-dichlorobenzaldehyde **2**, we followed the reaction kinetics by plotting the UV/vis absorbance versus time at a wavelength of 420 nm for the concentrations stated above to create the pseudo-order conditions. With respect to this value, the zero, first or second curve fittings were drawn automatically for the reaction using the software [30] associated with the UV/vis instrument. The original experimental absorbance against time data made a pseudo-first-order available fit curve at 420 nm, which exactly fits the experimental curve (dotted line) displayed in **Fig. 3**.

For this case, the rate law can be expressed as equations (2):

$$\text{Rate} = k_{\text{ovr}}[1]^{\alpha}[2]^{\beta}$$

$$\text{Rate} = k_{\text{obs}}[2]^{\beta} \quad (2)$$

$$k_{\text{ovr}} = \frac{k_{\text{obs}}}{[1]^{\alpha}} \quad (3)$$

It is obvious that the reaction is first order with respect to 2, 6-dichlorobenzaldehyde **2**, $\beta=1$. Whereas overall order of reaction is 2 ($\alpha+\beta=2$). Since $\beta=1$, it is reasonable to accept that the reaction is first-order with respect to compound **1** ($\alpha=1$).

Herein, the pseudo-first-order rate constants, k_{obs} were determined according to equation (3) by the software associated within the UV/vis instrument ($k_{\text{obs}}=0.1742$). By substituting the value of k_{obs} obtained from this experiment in equation (3) the value of k_{ovr} is achieved:

$$k_{\text{ovr}} = \frac{0.1742}{1 \times 10^{-2}} = 17.42$$

In fact, the obtained $k_{\text{ovr}}(17.42)$ from equation (3) in the third experiment is nearly equal to ($k_{\text{ovr}}=17.88 \text{ min}^{-1} \cdot \text{M}^{-1}$) obtained from the second experiment (equation (1)). This agreement also shows that the reaction is first order with respect to reactant **1** and indicates that α is one in equation (1).

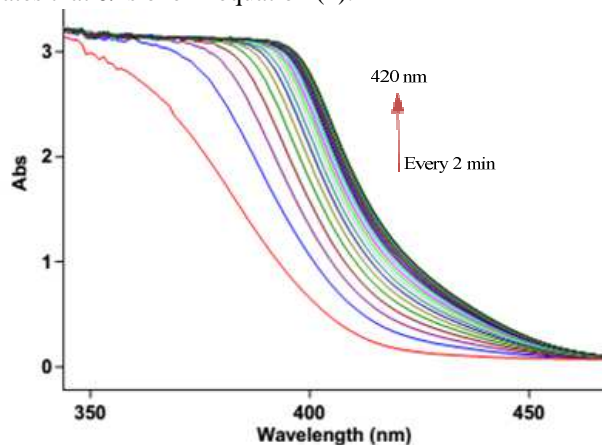


Fig. 2 Absorption changes versus wavelength for the reaction between **1** ($10^{-2} \text{ mol} \cdot \text{L}^{-1}$) and **2** ($10^{-2} \text{ mol} \cdot \text{L}^{-1}$) in formic acid for the generation of product **3** at 2 min intervals up to 30 min; the upward arrow indicates the direction of the reactions progress

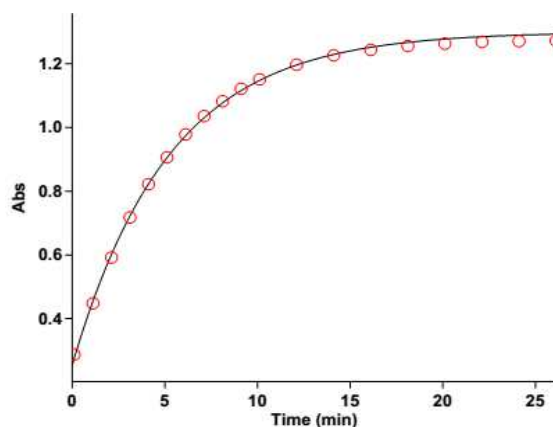


Fig. 3 The original experimental absorbance curve versus time at a selected wavelength of 420 nm for the reaction between 1 ($10^{-2} \text{ mol}\cdot\text{L}^{-1}$), and 2 ($10^{-2} \text{ mol}\cdot\text{L}^{-1}$) in formic acid. The dotted curve shows experimental values, and the solid line is the fitted curve

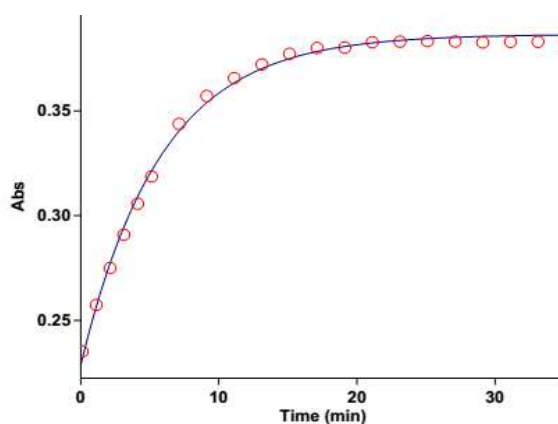


Fig. 4 The original experimental absorbance curve versus time (dotted line) along with the first pseudo order fit curve (solid line) in relation to 2, 6-dichlorobenzaldehyde 2 ($\beta=1$) for the reaction between 1 (10^{-2} M) and 2 (10^{-3} M) in formic acid

3.3 Solvents and temperature dependence of k_1

To determine the effect of in temperature change and solvent environment on the rate of reaction, it was elected to perform various experiments using different temperatures and solvent polarities but otherwise under same condition as the previous experiment. The effect of temperature on the rate of this reaction was studied in the range of 20–35°C. As shown in (Table. 2). The reaction rate increased along with increasing temperature, and the second-order rate constants of the reactions were obtained. Physical and chemical characteristics of solvents can cause variations in many reactions. To compare the effect of different solvents, solutions were prepared in various solvents. So, lone formic acid with a dielectric constant (58 D) and a mixture of acetic acid and formic acid (47.46 D, formic acid: acetic acid, 8:2) were chosen as suitable solvents. It can be observed that the rate constant (k_{ovr}) decreases in the presence of the solvents with a lower dielectric constant at all temperatures investigated and under same conditions (Table 2).

Table. 2 Reaction rate constants ($k_{\text{ovr}} \text{ M}^{-1}\cdot\text{min}^{-1}$) at different temperatures and solvents under the same conditions for the reaction between 1 ($10^{-2} \text{ mol}\cdot\text{L}^{-1}$) and 2 ($10^{-2} \text{ mol}\cdot\text{L}^{-1}$)

| Solvent | $k_{\text{ovr}}(\text{M}^{-1}\cdot\text{min}^{-1})$ | | | | | |
|--|---|----------------------|-------------------|-------------------|-------------------|-------------------|
| | $\epsilon(\text{D})$ | $\lambda(\text{nm})$ | 20°C | 25°C | 30°C | 35°C |
| formic acid | 58 | 420 | 12.88 (0.0017) | 17.88 (0.0008) | 35.01 (0.0311) | 51.99 (0.032) |
| mix formic acid / acetic acid (80:20) | 47.46 | 420 | 4.99 (0.0089) | 9.99 (0.0126) | 17.08 (0.0148) | 32.12 (0.0182) |

As can be seen in Table. 2 and Fig. 5, in the studied temperature range, the second-order rate constant ($\ln k_1$) of the reaction was inversely proportional to the temperature, which is in agreement with the Arrhenius equation:

$$\ln(k_{\text{ovr}}=k_1) = \ln A - \frac{E_a}{RT} \quad (4)$$

As shown in **Figure 5**, the apparent activation energy (E_a) in formic acid was calculated as ($72.84 \text{ kJ}\cdot\text{mol}^{-1}$) and in a mixture of solvent was ($91.89 \text{ kJ}\cdot\text{mol}^{-1}$). R , E_a and intercept ($\ln A$) of the straight line that best fits the points (**Fig. 5**). The higher activation energy ($E_a = 91.89 \text{ kJ}\cdot\text{mol}^{-1}$) was obtained in a mixture of solvent, while the value in formic acid was smaller, which means the reaction will occur more easily in the latter solvent. Two methods were used to estimate the activation energy. As expected, the results were approximately the same and the obtained values are given in (**Table. 3**) for both solvents. Eyring theory of reaction rates was used to evaluate the activation parameters involving ΔH^\ddagger and ΔS^\ddagger (**Fig. 6a**). The activation parameters were determined from the Eyring equation (5) and linearized form of the Eyring equation (6) [41, 42].

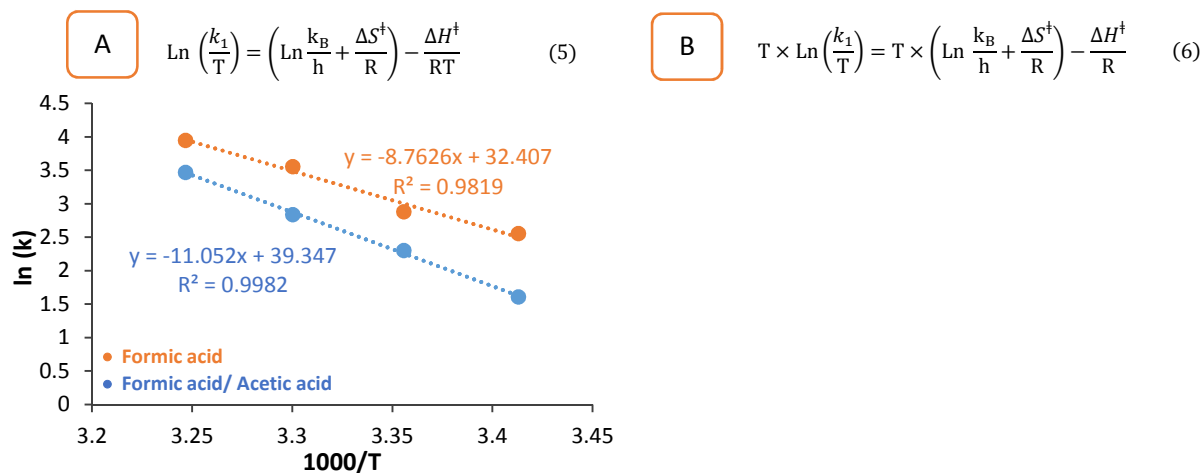


Fig. 5 Dependence of second order ($\ln k_{\text{ove}} = \ln k_i$) on reciprocal temperature for the reaction between reactants (1) and (2) in the presence of formic acid measured at a wavelength of 420 nm in accordance with the Arrhenius equation

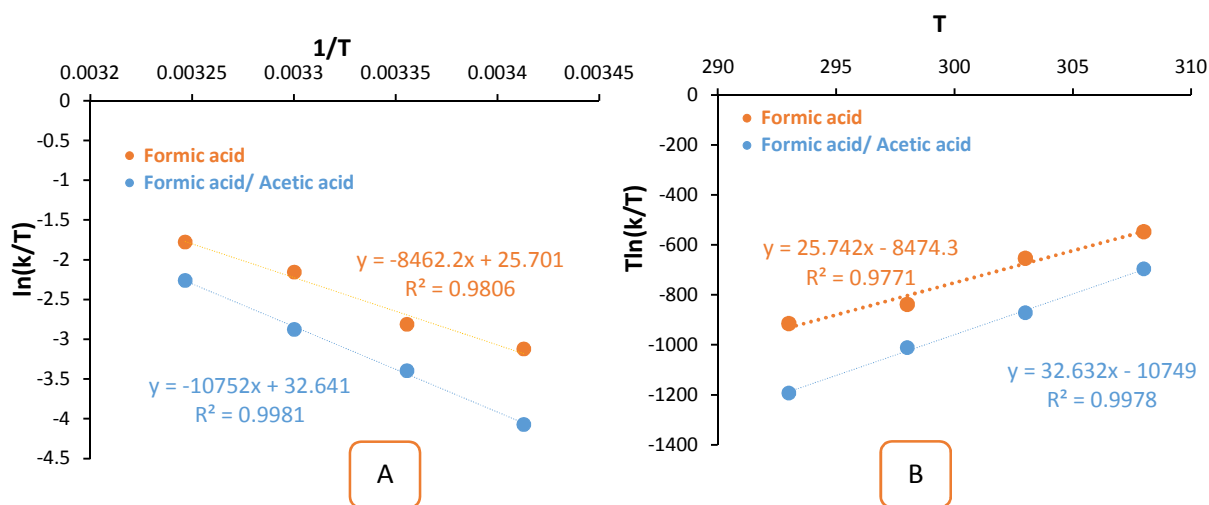


Fig. 6 A, B Eyring plots according to Eqs. (5) and (6) for the reaction between 1 and 2 in two different solvents at a wavelength of 420 nm

Two plots were drawn on the basis of the mentioned equations [(5) and (6)]. From the slopes and intercepts of these plots, the activation enthalpy and entropy were evaluated. A different linearized form of Eyring equation $\{T \ln(k_{\text{ovr}}/T) \text{ versus } T\}$ was examined (**Fig. 6B**) to check the comparison between the two methods [43]. As expected, the results were approximately the same and the obtained activation parameters are given in **Table. 3** for both solvents. It is inferred that the activation enthalpy in formic acid with a high reaction rate is less than in a mixture of formic acid/acetic acid. The positive activation entropy indicated a greater degree of ordering in the initial state than the transition state. These results suggest that in a mixture of solvent, the transition state is more disordered than in formic acid with respect to the ground state (**Table. 3**). The Gibbs free energy was determined using the Eq. (7):

$$\Delta G^\ddagger = \Delta H^\ddagger - T\Delta S^\ddagger \quad (7)$$

The Gibbs activation energy is essentially the energy requirement for a molecule to undergo the reaction. It is of interest to note that the activation Gibbs energies ΔG^\ddagger for both solvents are positive and the value of the activation Gibbs energy in formic acid is lower than that in a mixed solvent.

Table 3 Activation parameters (ΔS^\ddagger , ΔH^\ddagger and ΔG^\ddagger) using Eyring's equation and a linearized form (A from Eq. (5) and B from Eq. (6)) for the reaction between 1 ($10^{-2} \text{ mol}\cdot\text{L}^{-1}$) and 2 ($10^{-2} \text{ mol}\cdot\text{L}^{-1}$) in the presence of formic acid and mixed formic acid/acetic acid as a solvent

| Solvent | methods | ΔH^\ddagger | ΔS^\ddagger | ΔG^\ddagger | E_a |
|--|-------------------|-------------------------|--|-------------------------|-------------------------|
| | | (kJ.mol ⁻¹) | (J.mol ⁻¹ K ⁻¹) | (kJ.mol ⁻¹) | (kJ.mol ⁻¹) |
| formic acid | linearized form A | 70.45 | 16.47 | 65.54 | 72.84 ^a |
| | linearized form B | 70.35 | 16.13 | 65.54 | 72.88 ^b |
| A mixture of formic acid/acetic acid (20:80) | linearized form A | 89.36 | 73.76 | 67.38 | 91.89 ^a |
| | linearized form B | 89.39 | 73.83 | 67.39 | 91.79 ^b |

a: Calculated from Arrhenius Equation.

b: $E_a = \Delta H^\ddagger + RT$

When absorption spectra are measured in solvents of different polarity, it is found that the positions, intensities, and shapes of the absorption bands are usually modified by these solvents [44]. Most absorption spectroscopy of organic compounds is based on transitions of n or π electrons to the π^* excited state. This is because the absorption peaks for these transitions fall in an experimentally convenient region of the spectrum (200-500 nm). These transitions need an unsaturated group in the molecule to provide the π electrons. The UV/vis spectra of 2-(2, 6-dichlorophenyl)-2, 3-dihydroquinazolin-4(1H)-one are composed of $n-\pi^*$ and $\pi-\pi^*$ absorption bands, which show solvent effects; see **Fig. 7**. For the $n-\pi^*$ transition of this compound ($\lambda_{\text{max}} = 393 \text{ nm}$ in formic acid and $\lambda_{\text{max}} = 361 \text{ nm}$ in a mixture of formic acid/acetic acid), a big red shift of ($\Delta\lambda = 32 \text{ nm}$) is observed when going from a mixture of formic acid and acetic acid (8: 2) to formic acid as solvent. This big band shift is again mainly due to hydrogen bonding to the carbonyl group. Red shifts in $n-\pi^*$ transitions are caused mainly by dispersion effects. The excited state always has a larger polarizability than the ground state because an electron is promoted to a more diffuse orbital in which it is more polarizable. Thus the dispersion interaction of the excited solute with the solvent will be larger than the dispersion interaction of the ground-state solute with the solvent. The excitation energy decreases, resulting in a red shift. Incidentally, the $n-\pi^*$ transition energies of carbonyl groups in different solvents indicate the importance of the ground-state stabilization by solvents. Similarly, for $\pi-\pi^*$ absorption when going from a nonpolar to a polar solvent, the $\pi-\pi^*$ absorption also undergoes a bathochromic shift. This effect is greater for the excited state, and so the energy difference between the excited and unexcited states is slightly reduced resulting in a small red shift. This contradictory behavior of absorption bands along with changes for this reaction are shown in **Fig. 7(A, B)**.

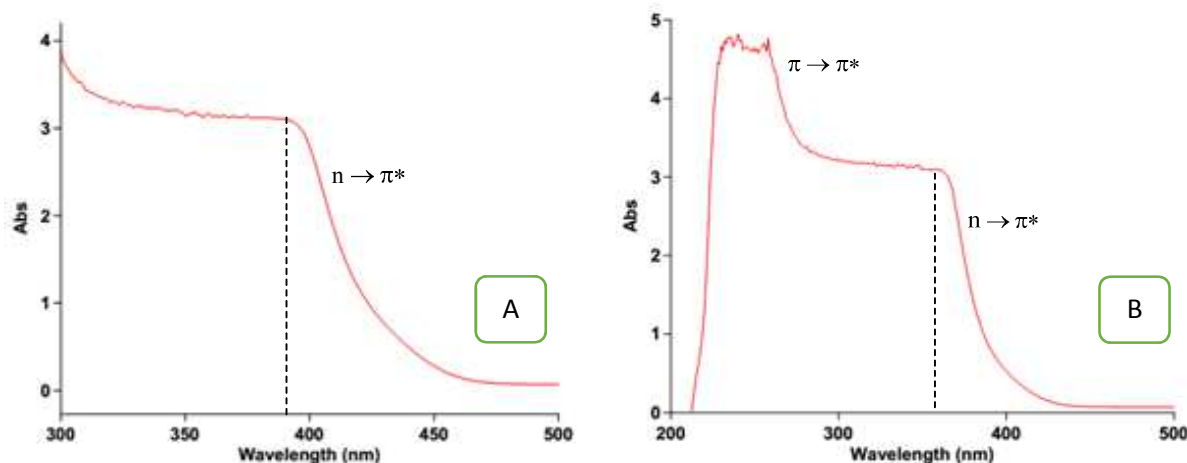


Fig. 7 A) Absorption changes versus wavelength and transfers occurrence for the reaction between 1 and 2 in formic acid for the generation of product 3. B) Absorption changes versus wavelength and transfers occurrence for the reaction between 1 and 2 in a mixture of formic acid and acetic acid (8:2)

3.3 Effect of catalyst

The reaction between 1 and 2 was accomplished in the presence of maltose as a second catalyst. The reaction rate was increased compared to formic acid (**Table 4**); that is, maltose has more interactions than formic acid, so, it can have more capability to carry out its catalytic role. According to results presented in **Table 4** maltose is a suitable catalyst for this reaction. Maltose, by creating hydrogen bonds with reagents, helps to speed up the rate of reaction. These hydrogen bonds are formed between maltose and oxygen of carbonyl group in 2, 6-dichlorobenzaldehyde. So with the formation of hydrogen bonds, free electron pair of nitrogen can easily to attack the carbonyl group, thus the reaction rate increased.

Table. 4 Effect of various catalysts on the reaction between 1 and 2 at 25°C and 420nm

| Catalyst | $k_{\text{obs}}(\text{M}\cdot\text{min}^{-1})$ | SD |
|-------------|--|--------|
| Formic acid | 17.88 | 0.0008 |
| Maltose | 21.07 | 0.022 |

4. Speculative Mechanism

Utilizing the above results, the simplified scheme of the proposed reaction mechanism (Fig. 8) is shown in Fig. 9.

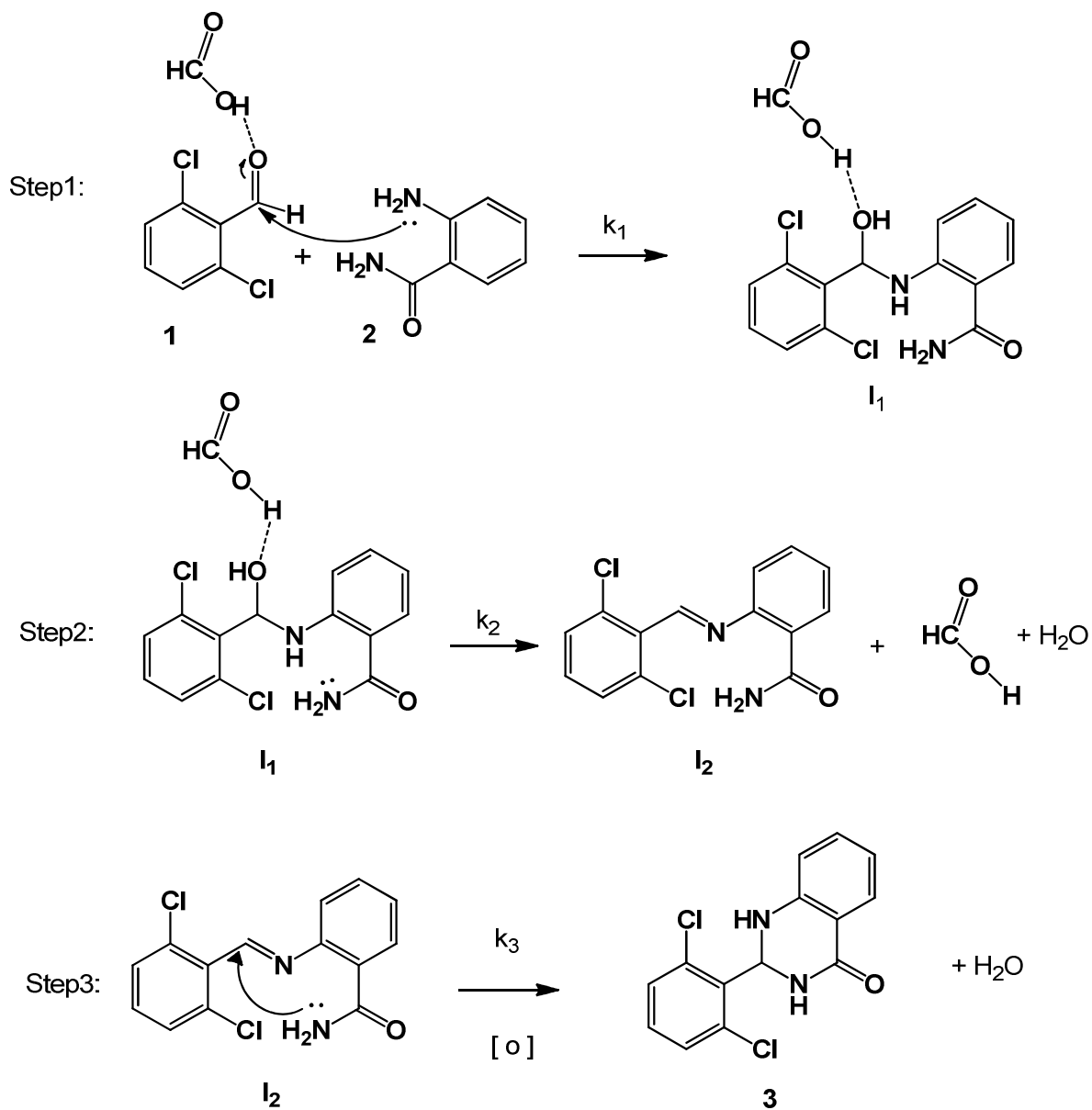


Fig. 8. The proposed reaction mechanism as a possible explanation for reaction between 1 and 2 in the presence of formic acid

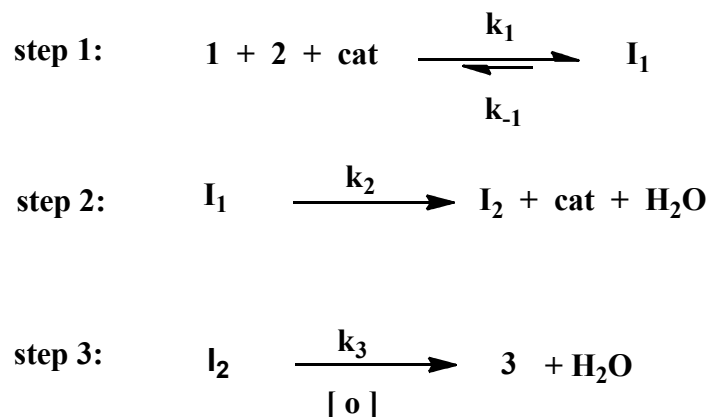


Fig. 9. The simplified scheme for the proposed reaction between 2, 6-dichlorobenzaldehyde 1 and 2-aminobenzamide 2 in the presence of formic acid as a solvent and catalyst

To investigate which steps of the proposed mechanism (Fig. 8) could be a rate determining step, the rate law is written using the final step for the product 3:

$$\text{rate} = k_3[I_2] \quad (8)$$

The steady state assumption can be employed for obtaining the concentration of $[I_2]$ which is generated from the following equations:

$$\frac{d[I_2]}{dt} = k_2[I_1] - k_3[I_2] = 0 \quad (9)$$

$$k_2[I_1] = k_3[I_2] \quad (10)$$

The value of equation (10) can be replaced in the equation (8) so the rate equation becomes:

$$\text{rate} = k_2[I_1] \quad (11)$$

For obtaining the concentration of intermediate $[I_1]$ the following equations were yielded by applying the steady state assumption:

$$\frac{d[I_1]}{dt} = k_1[1][2][\text{cat}] - k_{-1}[I_1] - k_2[I_1] = 0 \quad (12)$$

$$k_1[1][2][\text{cat}] = (k_{-1} + k_2)[I_1] \quad (13)$$

$$[I_1] = \frac{k_1 [1][2][\text{cat}]}{(k_{-1} + k_2)} = 0 \quad (14)$$

And with the placement of equation (14) in (11) the following equation is obtained:

$$\text{rate} = \frac{k_1 k_2 [1][2][\text{cat}]}{(k_{-1} + k_2)} \quad (15)$$

The following equation can be obtained:

$$k_{\text{ove}} = \frac{k_1 k_2}{(k_{-1} + k_2)} \quad (16)$$

$$\text{Rate} = k_{\text{ove}}[1][2] \quad (17)$$

The final equation (17) indicates that the overall order of the reaction is two which was formerly confirmed by the UV/vis experimental data. Herein, there are two possibilities for the RDS. Because of the absence of k_3 (step₃) in the rate law, this step could not be a rate determining step. For this reason, two possibilities for step₁ (k_1) and step₂ (k_2) were considered. If step₁ is a rate determining step, the assumption, $k_{-1} \ll k_2$, is reasonable, therefore the rate law can be expressed:

$$\text{Rate} = k_1[1][2] \quad (18)$$

That means the overall rate constant k_{ove} is exactly the same with the first rate constant: $k_1 = k_{\text{ove}}$. It would be good to remember that the first step is inherently a slow step. Effect of solvent generally that influences much more on the rate of slow step that has been observed in this work. Herein, experimental results (effect of solvent) practically indicated that the solvent with higher dielectric constant (formic acid, $D=58$) has a dipole-dipole interaction more with the transition state structure (Ts_1) with partial charges in comparison to reactant **1** and **2** with no charges. As a result, reduction of the activation energy speeds up the rate of reaction (see **Table. 3**).

If (step₂) is a rate determining step, the speculation, $k_{-1} \gg k_2$, is logical, so the rate law can be stated as:

$$\text{rate} = \frac{k_1 k_2 [1][2]}{(k_{-1})} \quad (19)$$

The new rate law is still the second order and in agreement with the results obtained by the UV/vis experiments. Herein, intermediate (I_1) participated lonely in step₂ for the elimination of H_2O , hence, this process which starts with an lone intermediate is inherently fast, particularly, in the presence of a protic solvent such as formic acid. As a result, equation (18) can be accepted as a rate law. On the basis of reports in other literatures [45], in the pH range near or above neutrality, imine formation (I_2), step₂ (k_2) is a rate determining step in the reaction mechanism, while in the acidic pH range, step₁ (k_1) is a rate determining step [35]. Herein in the presence of formic acid or a mixture of formic acid and acetic acid the reaction proceeds in the pH range below neutrality, thus the first step₁ (k_1) is a rate determining step.

CONCLUSION

Kinetic investigation of the recent reaction was undertaken using UV spectrophotometry technique. The results can be stated as follows:

1. The overall order of the reaction followed second-order kinetics and the reaction order of each reactant **2**, 6-dichlorobenzaldehyde **1**, and 2-aminobenzamid **2** is 1 and 1, respectively.
2. The overall rate constants of the reaction were calculated successfully at all investigated solvents and temperatures.
3. In solvents with higher dielectric constants, the rate of all reactions increased, and this could be related to the stabilization differences of the reactants and the activated complex by the solvent in the transition state (Ts_1 , step₁) of reaction mechanism.
4. Based on the experimental data, the first step of the suggested mechanism was identified as a rate-determining step (k_1) and this was confirmed by the steady state assumption, solvent investigation and reports in other literatures [35].
5. Activation energy ($72.84 \text{ kJ}\cdot\text{mol}^{-1}$) was calculated for the reaction in the formic acid and a mixture of formic acid /acetic acid.
6. In both solvent, the reaction is enthalpy controlled (ΔH^\ddagger is much greater than $T\Delta S^\ddagger$).

Acknowledgments

We gratefully acknowledge the financial support received from the Research Council of the University of Sistan and Baluchestan.

REFERENCES

- [1] M Sing; N. Raghav, *J. Bioorg. Chem.*, **2015**, 59, 12–22.
- [2] SM Roopan; FN Khan; JS Jin, *Pak. J. Pharm. Sci.*, **2013**, 26, 747–750.
- [3] Z Wang; M Wang; X Yao; Y Li; J Tan; L Wang; W Qiao; Y Geng; Y Liu; Q Wang, *Eur. J. Med. Chem.*, **2012**, 53, 275–282.
- [4] R Gali; J Banothu; M Porika; R Velpula; S Hnamte; R Bavantula; S Abbagani; S Busi, *Bioorg. Med. Chem. Lett.*, **2014**, 24, 4239–4242.
- [5] FA Cabrea-Rivera; J Escalante; H Morales-Rojas; DF zigler; RD Schmidt; LE Jarocha; MDE Forbes, *J. Photochem. Photobiol. A: Chem.*, **2014**, 294, 31-37.
- [6] MG Biressi; G Cantarelli; M Carissimi; A Cattaneo; F Ravenna, *Farmaco Ed. Sci.*, **1969**, 24,199.
- [7] M Bakavoli; O Sabzevari; M Rahimizadeh, *Chin. Chem. Lett.* **2007**, 18, 1466-1468.
- [8] JB Jiang; DP Hesson; BA Dusak; DL Dexter; GJ Kang; E Hamel, *J. Med. Chem.*, **1990**, 33, 1721.
- [9] K Hattori; Y Kido; H Yamamoto; J Ishida; K Kamijo; K Murano; M Ohkubo; T Kinoshita; A Iwashita; K Mihara; S Yamazaki; N Matsuoka; Y Teramura; H Miyake, *J Med. Chem.*, **2004**, 47, 4151.

- [10] HR Memarian; S Ebrahimi, *J Photochem. Photobiol, A: Chem.*, **2013**, 271, 8–15.
- [11] A Davoodnia; S Allameh; AR Fakhari; N Tavakoli-Hoseini, *Chin. Chem. Lett.*, **2010**, 21, 550–553.
- [12] M Dabiri; P Salehi; AA Mohammadi; M Baghbanzadeh; *Synth. Commun.*, **2005**, 35, 279–287.
- [13] X Xu; P Lu; Y Zhang, *Synth. Commun.*, **2001**, 31, 323–327.
- [14] N Montazeri; K Rad-Moghadam, Phosphoru, Sulfu, and Silicon., **2004**, 179, 2533–2536.
- [15] D Shi; L Rong; J Wang; Q Zhuang; X Wang; H Hu; *Synth. Commun.*, **2004**, 34, 1759–1765.
- [16] RJ Abdel-Jalil; W Voelter; M Saeed, *Tetrahedron Lett.*, 2004, 45, 3475–3476.
- [17] SD Sharma; V Kaur; *Synthesis.*, **1989**, 677.
- [18] JA Moore; GJ Sutherland; R Sowerby; EG Kelly; S Palermo; W Webster; *J. Org. Chem.*, **1969**, 887.
- [19] H Asakawa; M Matano; *Chem. Pharm. Bull.*, **1979**, 27, 1287.
- [20] G Cai; X Xu; Z Li; WP Weber; P Lu; *J. Heterocyclic Chem.*, **2002**, 39, 1271.
- [21] D Shi; L Rong; J Wang; Q Zhuang; X Wang; H Hu; *Tetrahedron Lett.*, **2003**, 44, 3199.
- [22] A Shaabani; A Maleki; H Mofakham, *Synth. Commun.*, **2008**, 38, 3751.
- [23] YX Zong; Y Zhao; WC Luo; XH Yu; JK Wang; Y Pan; *Chin. Chem. Lett.*, **2010**, 21, 778.
- [24] M Abdollahi-Alibeik; E Shabani, *Chin. Chem. Lett.* **2011**, 22, 1163.
- [26] P Salehi; M Dabiri; MA Zolfigol; M Baghbanzadeh, *Synth. Lett.*, **2005**, 16, 1155.
- [27] ZH Zhang; HY Lu; SH Yang; JW Gao; *J. Comb. Chem.*, **2010**, 12, 643.
- [28] J Chen; W Su; H Wu; M Liu; C Jin, *Green Chem.*, **2007**, 9, 972.
- [29] JA Moore; GJ Sutherland; R Sowerby; EG Kelly; S Palermo; W Webster, *J. Org. Chem.*, **1969**, 34, 887.
- [30] LM Schwartz; RI Gelb; *Anal. Chem.* **1978**, 50, 1592.
- [31] M Shahraki; SM Habibi-Khorassani, *J. Phys. Org. Chem.*, **2015**, 28(6), 396-402.
- [32] M Dehdab; SM Habibi-Khorassani; M Shahraki, *Catalysis Letters.*, **2014**, 144,1790.
- [33] M Shahraki; SM Habibi-Khorassani; M Dehdab, *RSC Adv.*, **2015**, 5, 52508-52515.
- [34] M Shahraki; SM Habibi-Khorassani; A Ebrahimi; MT Maghsoodlou; A Paknahad, *Prog. React. Kinet. Mech.*, **2012**, 37, 321.
- [35] SSh Pourpanah; SM Habibi-Khorassani; M Shahraki., *Chinese Journal of Catalysis.*, **2015**, 36, 757.
- [36] SM Habibi Khorassani; A Ebrahimi; MT Maghsoodlou; M Shahraki; D Price, *Analyst.*, **2011**,136, 1713.
- [37] SM Habibi-Khorassani; A Ebrahimi, MT Maghsoodlou, O Asheri, M Shahraki, N Akbarzadeh, Y Ghalandarzahi., *Int J Chem Kinet.*, **2013**, 45, 596.
- [38] SM Habibi-Khorassani; MT Maghsoodlou; M Shahraki; MA Poorshamsoddin; M Karima; M Abbasi, *Iranian journal of Catalysis.*, **2015**, 5, 79-87.
- [39] SM Habibi-Khorassani; MT Maghsoodlou; M Shahraki; M Hashemi-Shahri; J Aboonajmi; T Zarei, *Iranian journal of Catalysis.*, **2015**, 4, 241-246.
- [40] LM Schwartz; RI Gelb, *Anal. Chem.*, **1978**, 50, 1592.
- [41] JH Espenson, *Chemical kinetics and mechanisms*, 2nd edn. (McGraw-Hill, New York, **1995**).
- [42] A Poe, In: *mechanisms of Inorganic and Organometallic Reaction*, Vol. 8 ed. M.V. Twigg, (Plenum Press, New York), 220, **1994**.
- [43] G Lente; I Fabian; AJ Poe, *New J. Chem.*, **2005**, 29, 759.
- [44] C Reichardt, In: *Solvents and Solvent Effects in Organic Chemistry (Third Edition)*, WILEY-VCH Verlag GmbH & Co. KGaA, Weinheim, p. 329, **2003**.
- [45] JM Sayer; M Peskin; WP Jencks, *J. Am. Chem. Society.*, **1973**, 95, 4277–4287.